Measurement of the branching fraction, polarization, and CP asymmetries in $B^0 \to \rho^0 \rho^0$ decay, and implications for the CKM angle α

B. Aubert,[1] M. Bona,[1] Y. Karyotakis,[1] J. P. Lees,[1] V. Poireau,[1] E. Prencipe,[1] X. Prudent,[1] V. Tisserand,[1] J. Garra Tico,[2] E. Grauges,[2] L. Lopez,[3a,3b] A. Palano,[3a,3b] M. Pappagallo,[3a,3b] G. Eigen,[4] B. Stugu,[4] L. Sun,[4] G. S. Abrams,[5] M. Battaglia,[5] D. N. Brown,[5] R. N. Cahn,[5] R. G. Jacobsen,[5] L. T. Kerth,[5] Yu. G. Kolomensky,[5] G. Lynch,[5] I. L. Osipenkov,[5] M. T. Ronan,[5,*] K. Tackmann,[5] T. Tanabe,[5] C. M. Hawkes,[6] N. Soni,[6] A. T. Watson,[6] H. Koch,[7] T. Schroeder,[7] D. Walker,[8] D. J. Asgeirsson,[9] B. G. Fulsom,[9] C. Hearty,[9] T. S. Mattison,[9] J. A. McKenna,[9] M. Barrett,[10] A. Khan,[10] V. E. Blinov,[11] A. D. Bukin,[11] A. R. Buzykaev,[11] V. P. Druzhinin,[11] V. B. Golubev,[11] A. P. Onuchin,[11] S. I. Serednyakov,[11] Yu. I. Skovpen,[11] E. P. Solodov,[11] K. Yu. Todyshev,[11] M. Bondioli,[12] S. Curry,[12] I. Eschrich,[12] D. Kirkby,[12] A. J. Lankford,[12] P. Lund,[12] M. Mandelkern,[12] E. C. Martin,[12] D. P. Stoker,[12] S. Abachi,[13] C. Buchanan,[13] J. W. Gary,[14] F. Liu,[14] O. Long,[14] B. C. Shen,[14,*] G. M. Vitug,[14] Z. Yasin,[14] L. Zhang,[14] V. Sharma,[15] C. Campagnari,[16] T. M. Hong,[16] D. Kovalskyi,[16] M. A. Mazur,[16] J. D. Richman,[16] T. W. Beck,[17] A. M. Eisner,[17] C. J. Flacco,[17] C. A. Heusch,[17] J. Kroseberg,[17] W. S. Lockman,[17] A. J. Martinez,[17] T. Schalk,[17] B. A. Schumm,[17] A. Seiden,[17] M. G. Wilson,[17] L. O. Winstrom,[17] C. H. Cheng,[18] D. A. Doll,[18] B. Echenard,[18] F. Fang,[18] D. G. Hitlin,[18] I. Narsky,[18] T. Piatenko,[18] F. C. Porter,[18] R. Andreassen,[19] G. Mancinelli,[19] B. T. Meadows,[19] K. Mishra,[19] M. D. Sokoloff,[19] P. C. Bloom,[20] W. T. Ford,[20] A. Gaz,[20] J. F. Hirschauer,[20] M. Nagel,[20] U. Nauenberg,[20] J. G. Smith,[20] K. A. Ulmer,[20] S. R. Wagner,[20] R. Ayad,[21,+] A. Soffer,[21,‡] W. H. Toki,[21] R. J. Wilson,[21] D. D. Altenburg,[22] E. Feltresi,[22] A. Hauke,[22] H. Jasper,[22] M. Karbach,[22] J. Merkel,[22] A. Petzold,[22] B. Spaan,[22] K. Wacker,[22] M. J. Kobel,[23] W. F. Mader,[23] R. Nogowski,[23] K. R. Schubert,[23] R. Schwierz,[23] A. Volk,[23] D. Bernard,[24] G. R. Bonneaud,[24] E. Latour,[24] M. Verderi,[24] P. J. Clark,[25] S. Playfer,[25] J. E. Watson,[25] M. Andreotti,[26a,26b] D. Bettoni,[26a] C. Bozzi,[26a] R. Calabrese,[26a,26b] A. Cecchi,[26a,26b] G. Cibinetto,[26a,26b] P. Franchini,[26a,26b] E. Luppi,[26a,26b] M. Negrini,[26a,26b] A. Petrella,[26a,26b] L. Piemontese,[26a] V. Santoro,[26a,26b] R. Baldini-Ferroli,[27] A. Calcaterra,[27] R. de Sangro,[27] G. Finocchiaro,[27] S. Pacetti,[27] P. Patteri,[27] I. M. Peruzzi,[27,§] M. Piccolo,[27] M. Rama,[27] A. Zallo,[27] R. Contri,[28a,28b] M. Lo Vetere,[28a,28b] M. M. Macri,[28a] M. R. Monge,[28a,28b] S. Passaggio,[28a] C. Patrignani,[28a,28b] E. Robutti,[28a] A. Santroni,[28a,28b] S. Tosi,[28a,28b] K. S. Chaisanguanthum,[29] M. Morii,[29] A. Adametz,[30] J. Marks,[30] S. Schenk,[30] U. Uwer,[30] V. Klose,[31] H. M. Lacker,[31] D. J. Bard,[32] P. D. Dauncey,[32] J. A. Nash,[32] M. Tibbetts,[32] P. K. Behera,[33] X. Chai,[33] M. J. Charles,[33] U. Mallik,[33] J. Cochran,[34] H. B. Crawley,[34] L. Dong,[34] W. T. Meyer,[34] S. Prell,[34] E. I. Rosenberg,[34] A. E. Rubin,[34] Y. Y. Gao,[35] A. V. Gritsan,[35] Z. J. Guo,[35] C. K. Lae,[35] N. Arnaud,[36] J. Béquilleux,[36] A. D'Orazio,[36] M. Davier,[36] J. Firmino da Costa,[36] G. Grosdidier,[36] A. Höcker,[36] V. Lepeltier,[36] F. Le Diberder,[36] A. M. Lutz,[36] S. Pruvot,[36] P. Roudeau,[36] M. H. Schune,[36] J. Serrano,[36] V. Sordini,[36,‖] A. Stocchi,[36] G. Wormser,[36] D. J. Lange,[37] D. M. Wright,[37] I. Bingham,[38] J. P. Burke,[38] C. A. Chavez,[38] J. R. Fry,[38] E. Gabathuler,[38] R. Gamet,[38] D. E. Hutchcroft,[38] D. J. Payne,[38] C. Touramanis,[38] A. J. Bevan,[39] C. K. Clarke,[39] K. A. George,[39] F. Di Lodovico,[39] R. Sacco,[39] M. Sigamani,[39] G. Cowan,[40] H. U. Flaecher,[40] D. A. Hopkins,[40] S. Paramesvaran,[40] F. Salvatore,[40] A. C. Wren,[40] D. N. Brown,[41] C. L. Davis,[41] A. G. Denig,[42] M. Fritsch,[42] W. Gradl,[42] G. Schott,[42] K. E. Alwyn,[43] D. Bailey,[43] R. J. Barlow,[43] Y. M. Chia,[43] C. L. Edgar,[43] G. Jackson,[43] G. D. Lafferty,[43] T. J. West,[43] J. I. Yi,[43] J. Anderson,[44] C. Chen,[44] A. Jawahery,[44] D. A. Roberts,[44] G. Simi,[44] J. M. Tuggle,[44] C. Dallapiccola,[45] X. Li,[45] E. Salvati,[45] S. Saremi,[45] R. Cowan,[46] D. Dujmic,[46] P. H. Fisher,[46] G. Sciolla,[46] M. Spitznagel,[46] F. Taylor,[46] R. K. Yamamoto,[46] M. Zhao,[46] P. M. Patel,[47] S. H. Robertson,[47] A. Lazzaro,[48a,48b] V. Lombardo,[48a] F. Palombo,[48a,48b] J. M. Bauer,[49] L. Cremaldi,[49] R. Godang,[49,¶] R. Kroeger,[49] D. A. Sanders,[49] D. J. Summers,[49] H. W. Zhao,[49] M. Simard,[50] P. Taras,[50] F. B. Viaud,[50] H. Nicholson,[51] G. De Nardo,[52a,52b] L. Lista,[52a] D. Monorchio,[52a,52b] G. Onorato,[52a,52b] C. Sciacca,[52a,52b] G. Raven,[53] H. L. Snoek,[53] C. P. Jessop,[54] K. J. Knoepfel,[54] J. M. LoSecco,[54] W. F. Wang,[54] G. Benelli,[55] L. A. Corwin,[55] K. Honscheid,[55] H. Kagan,[55] R. Kass,[55] J. P. Morris,[55] A. M. Rahimi,[55] J. J. Regensburger,[55] S. J. Sekula,[55] Q. K. Wong,[55] N. L. Blount,[56] J. Brau,[56] R. Frey,[56] O. Igonkina,[56] J. A. Kolb,[56] M. Lu,[56] R. Rahmat,[56] N. B. Sinev,[56] D. Strom,[56] J. Strube,[56] E. Torrence,[56] G. Castelli,[57a,57b] N. Gagliardi,[57a,57b] M. Margoni,[57a,57b] M. Morandin,[57a] M. Posocco,[57a] M. Rotondo,[57a] F. Simonetto,[57a,57b] R. Stroili,[57a,57b] C. Voci,[57a,57b] P. del Amo Sanchez,[58] E. Ben-Haim,[58] H. Briand,[58] G. Calderini,[58] J. Chauveau,[58] P. David,[58] L. Del Buono,[58] O. Hamon,[58] Ph. Leruste,[58] J. Ocariz,[58] A. Perez,[58] J. Prendki,[58] S. Sitt,[58] L. Gladney,[59] M. Biasini,[60a,60b] R. Covarelli,[60a,60b] E. Manoni,[60a,60b] C. Angelini,[61a,61b] G. Batignani,[61a,61b] S. Bettarini,[61a,61b] M. Carpinelli,[61a,61b,**] A. Cervelli,[61a,61b] F. Forti,[61a,61b] M. A. Giorgi,[61a,61b] A. Lusiani,[61a,61c] G. Marchiori,[61a,61b] M. Morganti,[61a,61b] N. Neri,[61a,61b] E. Paoloni,[61a,61b] G. Rizzo,[61a,61b] J. J. Walsh,[61a] D. Lopes Pegna,[62] C. Lu,[62] J. Olsen,[62] A. J. S. Smith,[62] A. V. Telnov,[62] F. Anulli,[63a] E. Baracchini,[63a,63b] G. Cavoto,[63a] D. del Re,[63a,63b] E. Di Marco,[63a,63b] R. Faccini,[63a,63b]

F. Ferrarotto,[63a] F. Ferroni,[63a,63b] M. Gaspero,[63a,63b] P. D. Jackson,[63a] L. Li Gioi,[63a] M. A. Mazzoni,[63a] S. Morganti,[63a] G. Piredda,[63a] F. Polci,[63a,63b] F. Renga,[63a,63b] C. Voena,[63a] M. Ebert,[64] T. Hartmann,[64] H. Schröder,[64] R. Waldi,[64] T. Adye,[65] B. Franek,[65] E. O. Olaiya,[65] F. F. Wilson,[65] S. Emery,[66] M. Escalier,[66] L. Esteve,[66] S. F. Ganzhur,[66] G. Hamel de Monchenault,[66] W. Kozanecki,[66] G. Vasseur,[66] Ch. Yèche,[66] M. Zito,[66] X. R. Chen,[67] H. Liu,[67] W. Park,[67] M. V. Purohit,[67] R. M. White,[67] J. R. Wilson,[67] M. T. Allen,[68] D. Aston,[68] R. Bartoldus,[68] P. Bechtle,[68] J. F. Benitez,[68] R. Cenci,[68] J. P. Coleman,[68] M. R. Convery,[68] J. C. Dingfelder,[68] J. Dorfan,[68] G. P. Dubois-Felsmann,[68] W. Dunwoodie,[68] R. C. Field,[68] A. M. Gabareen,[68] S. J. Gowdy,[68] M. T. Graham,[68] P. Grenier,[68] C. Hast,[68] W. R. Innes,[68] J. Kaminski,[68] M. H. Kelsey,[68] H. Kim,[68] P. Kim,[68] M. L. Kocian,[68] D. W. G. S. Leith,[68] S. Li,[68] B. Lindquist,[68] S. Luitz,[68] V. Luth,[68] H. L. Lynch,[68] D. B. MacFarlane,[68] H. Marsiske,[68] R. Messner,[68] D. R. Muller,[68] H. Neal,[68] S. Nelson,[68] C. P. O'Grady,[68] I. Ofte,[68] A. Perazzo,[68] M. Perl,[68] B. N. Ratcliff,[68] A. Roodman,[68] A. A. Salnikov,[68] R. H. Schindler,[68] J. Schwiening,[68] A. Snyder,[68] D. Su,[68] M. K. Sullivan,[68] K. Suzuki,[68] S. K. Swain,[68] J. M. Thompson,[68] J. Va'vra,[68] A. P. Wagner,[68] M. Weaver,[68] C. A. West,[68] W. J. Wisniewski,[68] M. Wittgen,[68] D. H. Wright,[68] H. W. Wulsin,[68] A. K. Yarritu,[68] K. Yi,[68] C. C. Young,[68] V. Ziegler,[68] P. R. Burchat,[69] A. J. Edwards,[69] S. A. Majewski,[69] T. S. Miyashita,[69] B. A. Petersen,[69] L. Wilden,[69] S. Ahmed,[70] M. S. Alam,[70] J. A. Ernst,[70] B. Pan,[70] M. A. Saeed,[70] S. B. Zain,[70] S. M. Spanier,[71] B. J. Wogsland,[71] R. Eckmann,[72] J. L. Ritchie,[72] A. M. Ruland,[72] C. J. Schilling,[72] R. F. Schwitters,[72] B. W. Drummond,[73] J. M. Izen,[73] X. C. Lou,[73] F. Bianchi,[74a,74b] D. Gamba,[74a,74b] M. Pelliccioni,[74a,74b] M. Bomben,[75a,75b] L. Bosisio,[75a,75b] C. Cartaro,[75a,75b] G. Della Ricca,[75a,75b] L. Lanceri,[75a,75b] L. Vitale,[75a,75b] V. Azzolini,[76] N. Lopez-March,[76] F. Martinez-Vidal,[76] D. A. Milanes,[76] A. Oyanguren,[76] J. Albert,[77] Sw. Banerjee,[77] B. Bhuyan,[77] H. H. F. Choi,[77] K. Hamano,[77] R. Kowalewski,[77] M. J. Lewczuk,[77] I. M. Nugent,[77] J. M. Roney,[77] R. J. Sobie,[77] T. J. Gershon,[78] P. F. Harrison,[78] J. Ilic,[78] T. E. Latham,[78] G. B. Mohanty,[78] H. R. Band,[79] X. Chen,[79] S. Dasu,[79] K. T. Flood,[79] Y. Pan,[79] M. Pierini,[79] R. Prepost,[79] C. O. Vuosalo,[79] and S. L. Wu[79]

(*BABAR* Collaboration)

[1]*Laboratoire de Physique des Particules, IN2P3/CNRS et Université de Savoie, F-74941 Annecy-Le-Vieux, France*
[2]*Universitat de Barcelona, Facultat de Fisica, Departament ECM, E-08028 Barcelona, Spain*
[3a]*INFN Sezione di Bari, I-70126 Bari, Italy*
[3b]*Dipartimento di Fisica, Università di Bari, I-70126 Bari, Italy*
[4]*University of Bergen, Institute of Physics, N-5007 Bergen, Norway*
[5]*Lawrence Berkeley National Laboratory and University of California, Berkeley, California 94720, USA*
[6]*University of Birmingham, Birmingham, B15 2TT, United Kingdom*
[7]*Ruhr Universität Bochum, Institut für Experimentalphysik 1, D-44780 Bochum, Germany*
[8]*University of Bristol, Bristol BS8 1TL, United Kingdom*
[9]*University of British Columbia, Vancouver, British Columbia, Canada V6T 1Z1*
[10]*Brunel University, Uxbridge, Middlesex UB8 3PH, United Kingdom*
[11]*Budker Institute of Nuclear Physics, Novosibirsk 630090, Russia*
[12]*University of California at Irvine, Irvine, California 92697, USA*
[13]*University of California at Los Angeles, Los Angeles, California 90024, USA*
[14]*University of California at Riverside, Riverside, California 92521, USA*
[15]*University of California at San Diego, La Jolla, California 92093, USA*
[16]*University of California at Santa Barbara, Santa Barbara, California 93106, USA*
[17]*University of California at Santa Cruz, Institute for Particle Physics, Santa Cruz, California 95064, USA*
[18]*California Institute of Technology, Pasadena, California 91125, USA*
[19]*University of Cincinnati, Cincinnati, Ohio 45221, USA*
[20]*University of Colorado, Boulder, Colorado 80309, USA*
[21]*Colorado State University, Fort Collins, Colorado 80523, USA*
[22]*Technische Universität Dortmund, Fakultät Physik, D-44221 Dortmund, Germany*
[23]*Technische Universität Dresden, Institut für Kern- und Teilchenphysik, D-01062 Dresden, Germany*
[24]*Laboratoire Leprince-Ringuet, CNRS/IN2P3, Ecole Polytechnique, F-91128 Palaiseau, France*
[25]*University of Edinburgh, Edinburgh EH9 3JZ, United Kingdom*
[26a]*INFN Sezione di Ferrara, I-44100 Ferrara, Italy*
[26b]*Dipartimento di Fisica, Università di Ferrara, I-44100 Ferrara, Italy*
[27]*INFN Laboratori Nazionali di Frascati, I-00044 Frascati, Italy*
[28a]*INFN Sezione di Genova, I-16146 Genova, Italy*
[28b]*Dipartimento di Fisica, Università di Genova, I-16146 Genova, Italy*
[29]*Harvard University, Cambridge, Massachusetts 02138, USA*

[30]Universität Heidelberg, Physikalisches Institut, Philosophenweg 12, D-69120 Heidelberg, Germany

[31]Humboldt-Universität zu Berlin, Institut für Physik, Newtonstr. 15, D-12489 Berlin, Germany

[32]Imperial College London, London, SW7 2AZ, United Kingdom

[33]University of Iowa, Iowa City, Iowa 52242, USA

[34]Iowa State University, Ames, Iowa 50011-3160, USA

[35]Johns Hopkins University, Baltimore, Maryland 21218, USA

[36]Laboratoire de l'Accélérateur Linéaire, IN2P3/CNRS et Université Paris-Sud 11, Centre Scientifique d'Orsay,
B. P. 34, F-91898 Orsay Cedex, France

[37]Lawrence Livermore National Laboratory, Livermore, California 94550, USA

[38]University of Liverpool, Liverpool L69 7ZE, United Kingdom

[39]Queen Mary, University of London, London, E1 4NS, United Kingdom

[40]University of London, Royal Holloway and Bedford New College, Egham, Surrey TW20 0EX, United Kingdom

[41]University of Louisville, Louisville, Kentucky 40292, USA

[42]Johannes Gutenberg-Universität Mainz, Institut für Kernphysik, D-55099 Mainz, Germany

[43]University of Manchester, Manchester M13 9PL, United Kingdom

[44]University of Maryland, College Park, Maryland 20742, USA

[45]University of Massachusetts, Amherst, Massachusetts 01003, USA

[46]Massachusetts Institute of Technology, Laboratory for Nuclear Science, Cambridge, Massachusetts 02139, USA

[47]McGill University, Montréal, Québec, Canada H3A 2T8

[48a]INFN Sezione di Milano, I-20133 Milano, Italy

[48b]Dipartimento di Fisica, Università di Milano, I-20133 Milano, Italy

[49]University of Mississippi, University, Mississippi 38677, USA

[50]Université de Montréal, Physique des Particules, Montréal, Québec, Canada H3C 3J7

[51]Mount Holyoke College, South Hadley, Massachusetts 01075, USA

[52a]INFN Sezione di Napoli, I-80126 Napoli, Italy

[52b]Dipartimento di Scienze Fisiche, Università di Napoli Federico II, I-80126 Napoli, Italy

[53]NIKHEF, National Institute for Nuclear Physics and High Energy Physics, NL-1009 DB Amsterdam, The Netherlands

[54]University of Notre Dame, Notre Dame, Indiana 46556, USA

[55]Ohio State University, Columbus, Ohio 43210, USA

[56]University of Oregon, Eugene, Oregon 97403, USA

[57a]INFN Sezione di Padova, I-35131 Padova, Italy

[57b]Dipartimento di Fisica, Università di Padova, I-35131 Padova, Italy

[58]Laboratoire de Physique Nucléaire et de Hautes Energies, IN2P3/CNRS, Université Pierre et Marie Curie-Paris6,
Université Denis Diderot-Paris7, F-75252 Paris, France

[59]University of Pennsylvania, Philadelphia, Pennsylvania 19104, USA

[60a]INFN Sezione di Perugia, I-06100 Perugia, Italy

[60b]Dipartimento di Fisica, Università di Perugia, I-06100 Perugia, Italy

[61a]INFN Sezione di Pisa, I-56127 Pisa, Italy

[61b]Dipartimento di Fisica, Università di Pisa, I-56127 Pisa, Italy

[61c]Scuola Normale Superiore di Pisa, I-56127 Pisa, Italy

[62]Princeton University, Princeton, New Jersey 08544, USA

[63a]INFN Sezione di Roma, I-00185 Roma, Italy

[63b]Dipartimento di Fisica, Università di Roma La Sapienza, I-00185 Roma, Italy

[64]Universität Rostock, D-18051 Rostock, Germany

[65]Rutherford Appleton Laboratory, Chilton, Didcot, Oxon, OX11 0QX, United Kingdom

[66]CEA, Irfu, SPP, Centre de Saclay, F-91191 Gif-sur-Yvette, France

[67]University of South Carolina, Columbia, South Carolina 29208, USA

[68]Stanford Linear Accelerator Center, Stanford, California 94309, USA

[69]Stanford University, Stanford, California 94305-4060, USA

[70]State University of New York, Albany, New York 12222, USA

[71]University of Tennessee, Knoxville, Tennessee 37996, USA

[72]University of Texas at Austin, Austin, Texas 78712, USA

---

[*]Deceased.

[+]Now at Temple University, Philadelphia, PA 19122, USA.

[‡]Now at Tel Aviv University, Tel Aviv, 69978, Israel.

[§]Also with Università di Perugia, Dipartimento di Fisica, Perugia, Italy.

[‖]Also with Università di Roma La Sapienza, I-00185 Roma, Italy.

[¶]Now at University of South Alabama, Mobile, AL 36688, USA.

[**]Also with Università di Sassari, Sassari, Italy.

[73]*University of Texas at Dallas, Richardson, Texas 75083, USA*
[74a]*INFN Sezione di Torino, I-10125 Torino, Italy*
[74b]*Dipartimento di Fisica Sperimentale, Università di Torino, I-10125 Torino, Italy*
[75a]*INFN Sezione di Trieste, I-34127 Trieste, Italy*
[75b]*Dipartimento di Fisica, Università di Trieste, I-34127 Trieste, Italy*
[76]*IFIC, Universitat de Valencia-CSIC, E-46071 Valencia, Spain*
[77]*University of Victoria, Victoria, British Columbia, Canada V8W 3P6*
[78]*Department of Physics, University of Warwick, Coventry CV4 7AL, United Kingdom*
[79]*University of Wisconsin, Madison, Wisconsin 53706, USA*

We study $B^0 \to \rho^0\rho^0$ decays in a sample of 465×10^6 $\Upsilon(4S) \to B\bar{B}$ events collected with the *BABAR* detector at the PEP-II asymmetric-energy e^+e^- collider located at the Stanford Linear Accelerator Center (SLAC). We measure the branching fraction $\mathcal{B} = (0.92 \pm 0.32 \pm 0.14) \times 10^{-6}$ and longitudinal polarization fraction $f_L = 0.75^{+0.11}_{-0.14} \pm 0.05$, where the first uncertainty is statistical and the second is systematic. The evidence for the $B^0 \to \rho^0\rho^0$ signal has a significance of 3.1 standard deviations, including systematic uncertainties. We investigate the proper-time dependence of the longitudinal component in the decay and measure the *CP*-violating coefficients $S_L^{00} = (0.3 \pm 0.7 \pm 0.2)$ and $C_L^{00} = (0.2 \pm 0.8 \pm 0.3)$. We study the implication of these results for the unitarity triangle angle α.

Measurements of *CP*-violating asymmetries test the flavor structure of the standard model by overconstraining the Cabibbo-Kobayashi-Maskawa (CKM) quark-mixing matrix [1]. The time-dependent *CP* asymmetry in the decays of B^0 or $\bar{B}^0$ mesons to a *CP* eigenstate dominated by the tree-level amplitude $b \to u\bar{u}d$ measures $\sin 2\alpha_{\mathrm{eff}}$, where α_{eff} differs from the CKM unitarity triangle angle $\alpha \equiv \arg[-V_{td}V_{tb}^*/V_{ud}V_{ub}^*]$ by a quantity $\Delta\alpha$ accounting for the contributions from loop (penguin) amplitudes. The value of $\Delta\alpha$ can be extracted from an analysis of the full set of isospin-related channels [2].

Since the tree contribution to the $B^0 \to \rho^0\rho^0$ [3] decay is color suppressed, the decay rate is much smaller than those of the $B^0 \to \rho^+\rho^-$ and $B^+ \to \rho^+\rho^0$ channels [4–8], and is sensitive to the penguin amplitude. Therefore a stringent limit on $\Delta\alpha$ can be set [2,7,9]. This makes the $\rho\rho$ system particularly effective for measuring α.

In $B \to \rho\rho$ decays the final state is a superposition of *CP*-odd and *CP*-even states. An isospin-triangle relation [2] holds for each of the three helicity amplitudes $A_{\lambda=-1,0,+1}$, which can be separated through an angular analysis. The longitudinal polarization fraction $f_L = |A_0|^2/\sum|A_\lambda|^2$ can be determined through the measurement of the distribution of the helicity angles θ_1 and θ_2, defined as the angles between the direction of the π^+ and the direction of the B meson in the rest system of each of the $\rho^0 \to \pi^+\pi^-$ candidates.

In this paper, we update our previous measurement [4] of the branching fraction $\mathcal{B}$ and longitudinal polarization fraction f_L in $B^0 \to \rho^0\rho^0$ decays, along with $\mathcal{B}$ for $B^0 \to \rho^0 f_0$, $f_0 f_0$, $\rho^0\pi^+\pi^-$, and $\pi^+\pi^-\pi^+\pi^-$. In addition, we present the first study of the time-dependent *CP* asymmetry $\mathcal{A}_{CP}$ in this mode. We determine the coefficients C_L^{00} and S_L^{00} of $\mathcal{A}_{CP}$ for the longitudinal component, expressed as a function of Δt, the proper-time difference between the

two B decays in $\Upsilon(4S) \to B^0\bar{B}^0$:

$$\mathcal{A}_{CP}(\Delta t) = -C_L^{00}\cos\Delta m\Delta t + S_L^{00}\sin\Delta m\Delta t, \quad (1)$$

where $\Delta m = (0.507 \pm 0.005)\hbar\,\mathrm{ps}^{-1}$ is the mass difference between two B^0 mass eigenstates [10]. When combined with measurements of $B^0 \to \rho^+\rho^-$ and $B^+ \to \rho^+\rho^0$, $\mathcal{A}_{CP}$, $\mathcal{B}$, and f_L in $B^0 \to \rho^0\rho^0$ allow a complete isospin analysis and improve the constraints on the penguin contribution to $B \to \rho\rho$ decays. Changes with respect to our previous analysis [4] include a larger data sample, improved track selection and reconstruction techniques, inclusion of the *B*-decay time information, and improved handling of background events originating from B decays.

We use a sample of $(465 \pm 5) \times 10^6$ $\Upsilon(4S)$ decays into $B\bar{B}$ pairs collected with the *BABAR* detector [11] at the PEP-II asymmetric-energy e^+e^- collider [12]. A detailed description of the *BABAR* detector is available elsewhere [4,11].

We select $B \to M_1 M_2 \to (\pi^+\pi^-)(\pi^+\pi^-)$ candidates, where $M_{1,2}$ stands for a ρ^0 or $f_0(980)$ candidate, from neutral combinations of four charged tracks that are consistent with originating from a single vertex near the e^+e^- interaction point. We veto tracks that are positively identified as kaons or electrons. The identification of signal B candidates is based on several kinematic variables. The beam-energy-substituted mass $m_{\mathrm{ES}} = [(s/2 + \mathbf{p}_i \cdot \mathbf{p}_B)^2/E_i^2 - \mathbf{p}_B^2]^{1/2}$, where the initial e^+e^- four-momentum $(E_i, \mathbf{p}_i)$ and the B momentum $\mathbf{p_B}$ are defined in the laboratory frame, is centered near the B mass with a resolution of 2.6 MeV/c^2 for signal candidates. The difference $\Delta E = E_B^{\mathrm{cm}} - \sqrt{s}/2$ between the reconstructed B energy in the center of mass (c.m.) frame and its known value $\sqrt{s}/2$ has a maximum near zero with a resolution of 20 MeV for signal events. Four other kinematic variables describe two pos-

sible $\pi^+\pi^-$ pairs: invariant masses m_1, m_2 and helicity angles θ_1, θ_2.

We use the kinematic selection of signal candidates described in [4]. We require $5.245 < m_{ES} < 5.290$ GeV/c^2, $|\Delta E| < 85$ MeV, $0.55 < m_{1,2} < 1.050$ GeV/c^2, and $|\cos\theta_{1,2}| < 0.98$. The extended dipion invariant mass range allows us to study the nonresonant decays $B^0 \to \rho^0\pi^+\pi^-$ and $B^0 \to \pi^+\pi^-\pi^+\pi^-$, as well as $B^0 \to \rho^0 f_0$ and $B^0 \to f_0 f_0$. The contributions from the higher mass resonances in this range are relatively small. We suppress the dominant $e^+e^- \to q\bar{q}$ ($q = u, d, s, c$) continuum background using a neural network-based discriminant $\mathcal{E}$, which combines eight topological variables [4].

We use multivariate B-flavor tagging algorithms trained to identify primary leptons, kaons, soft pions, and high-momentum charged particles from the other B, called B_{tag} [13]. The effective tagging efficiency is $(31.1 \pm 0.3)\%$. Additional background discrimination power arises from the difference between the tagging efficiencies for signal and background in seven tagging categories (c_{tag}). We determine Δt and its error $\sigma_{\Delta t}$ from the spatial separation between the decay vertices of the signal B and B_{tag} and require $|\Delta t| < 15$ ps and $\sigma_{\Delta t} < 2.5$ ps.

After application of all selection criteria, 72 154 events are retained. On average, each selected event has 1.05 signal candidates, while in Monte Carlo (MC) [14,15] samples of longitudinally (transversely) polarized $B^0 \to \rho^0\rho^0$ decays, we find 1.15 (1.03) candidates. When more than one candidate is present in the same event, the candidate that yields the smallest χ^2 for the four-pion vertex is selected. Simulation shows that 18% of longitudinally and 4% of transversely polarized $B^0 \to \rho^0\rho^0$ events are misreconstructed with one or more tracks that do not originate from the $B^0 \to \rho^0\rho^0$ decay. These are mostly low-momentum tracks from the other B meson in the event. Such partially reconstructed candidates are included in the definition of the signal probability density functions (PDFs). The rate of events in which all pions from $B^0 \to [\pi^+\pi^-]_\rho[\pi^+\pi^-]_\rho$ are found but incorrectly paired in the ρ^0 candidates is negligibly small.

We use an unbinned extended maximum likelihood fit to extract the $B^0 \to \rho^0\rho^0$ event yield, f_L, C_L^{00}, and S_L^{00}. We also fit for the event yields of $B^0 \to \rho^0 f_0$, $B^0 \to f_0 f_0$, $B^0 \to \rho^0\pi^+\pi^-$, and $B^0 \to \pi^+\pi^-\pi^+\pi^-$ decays. The likelihood function includes the background components from nonsignal B decays and continuum. The PDFs for each component depend on ten discriminating variables: m_{ES}, ΔE, $\mathcal{E}$, m_1, m_2, $\cos\theta_1$, $\cos\theta_2$, c_{tag}, Δt, and $\sigma_{\Delta t}$.

Since the statistical correlations among the variables are found to be negligibly small, we take the total PDF as the product of the PDFs for the separate variables. Exceptions are the kinematic correlation between the two helicity angles in signal, and mass-helicity correlations in several B-decay classes and misreconstructed signal.

We use double-Gaussian functions to parametrize the m_{ES} and ΔE PDFs for signal, and relativistic Breit-Wigner functions for the resonance line shapes of ρ^0 and $f_0(980)$, with the $f_0(980)$ mass and width taken from [16]. The angular distribution for B decays [14] (expressed as a function of f_L for $B^0 \to \rho^0\rho^0$) is multiplied by a detector acceptance function determined from simulations. We assume that the ρ^0 in $B^0 \to \rho^0\pi^+\pi^-$ is longitudinally polarized (i.e., $\pi^+\pi^-$ are produced in the S wave), and we use the phase-space distributions for $B^0 \to \pi^+\pi^-\pi^+\pi^-$. The $(\pi\pi)$ invariant mass and helicity distributions of misreconstructed signal events are parametrized with empirical shapes in a way similar to that used for B background discussed below. The neural network discriminant $\mathcal{E}$ is described by the sum of three asymmetric Gaussian functions with different parameters for signal and background distributions.

The PDFs for nonsignal B-decay modes are generally modeled with empirical analytical distributions. Several variables have distributions identical to those for signal, such as m_{ES} when all four tracks come from the same B, or $m_{1,2}$ when both tracks come from a ρ^0 meson. Also, for some of the modes the two $\pi^+\pi^-$ pairs can have different mass and helicity distributions, e.g., when only one of the two combinations comes from a genuine ρ^0 or f_0 meson, or when one of the two pairs contains a high-momentum pion (as in $B \to a_1\pi$). In such cases, we use a four-variable correlated mass-helicity PDF. The proper-time distribution for signal and background B decays is convolved with a resolution function [13], while the time distribution of continuum background is assumed to have zero lifetime.

The signal and B-background PDF parameters are extracted from simulation. The MC parameters for the m_{ES}, ΔE, and $\mathcal{E}$ PDFs are adjusted by comparing data and simulation in control channels with similar kinematics and topology, such as $B^0 \to D^-\pi^+$ with $D^- \to K^+\pi^-\pi^-$. The continuum background PDF shapes are extracted from on-resonance sideband data ($m_{ES} < 5.27$ GeV/c^2), with parameters of most PDFs (for m_{ES}, ΔE, $\mathcal{E}$, θ_1, θ_2, and Δt) left free in the final fit. The tagging efficiencies, mistag fractions, and the parameters of the proper-time distributions for signal modes are obtained in dedicated fits to events with identified exclusive B decays [13]. For inclusive B backgrounds these parameters are determined by MC and their systematic uncertainties are evaluated in data.

We study the contributions of the dominant backgrounds by using high-statistics exclusive MC samples. We single out the $B^0 \to a_1^\pm\pi^\mp$, $B^0 \to \rho^0 K^{*0}$, and $B^0 \to f_0 K^{*0}$ modes, which have kinematic distributions similar to those of the signal events, and parametrize their PDFs individually. The event yield for $B^0 \to a_1^\pm\pi^\mp$ is allowed to vary in the fit, while the yields for $B^0 \to \rho^0 K^{*0}$, $B^0 \to f_0 K^{*0}$ are fixed to the expected values [17].

TABLE I. Event yields; fraction of longitudinal polarization (f_L); selection efficiency corresponding to measured polarization; branching fractions ($\mathcal{B}$); branching fraction upper limits at 90% confidence level (CL); and significance $\mathcal{S}$ including systematic uncertainties. The first uncertainty is statistical and the second is systematic.

Mode	Yield	f_L	Efficiency (%)	$\mathcal{B}$ (10^{-6})	Upper limit (10^{-6})	$\mathcal{S}$ (σ)
$B^0 \to \rho^0\rho^0$	$99^{+35}_{-34} \pm 15$	$0.75^{+0.11}_{-0.14} \pm 0.05$	23.28 ± 0.07	$0.92 \pm 0.32 \pm 0.14$	$\cdots$	3.1
$B^0 \to \rho^0 f_0 \to \rho^0[\pi^+\pi^-]_{f_0}$	$3^{+22}_{-20} \pm 12$	$\cdots$	24.16 ± 0.09	$0.03 \pm 0.19 \pm 0.10$	<0.40	
$B^0 \to f_0 f_0 \to [\pi^+\pi^-]_{f_0}[\pi^+\pi^-]_{f_0}$	$7^{+8}_{-5} \pm 7$	$\cdots$	27.22 ± 0.07	$0.05^{+0.06}_{-0.04} \pm 0.05$	<0.19	
$B^0 \to \rho^0\pi^+\pi^-$	$-13^{+39}_{-35} \pm 18$	$\cdots$	1.68 ± 0.01	$-1.6^{+5.0}_{-4.5} \pm 2.2$	<8.8	
$B^0 \to \pi^+\pi^-\pi^+\pi^-$	$8^{+30}_{-25} \pm 11$	$\cdots$	0.55 ± 0.01	$3.0^{+11.6}_{-9.9} \pm 4.1$	<23.1	

In addition, we construct a charmless event category consisting of $B^0 \to \rho^+\rho^-$, $B^0 \to \rho^\pm\pi^\mp$, $B^+ \to \rho^+\rho^0$, $B^+ \to a_1^0\pi^+$, $B^+ \to a_1^+ f_0$, $B \to \eta' K$, and $B^+ \to \rho^0\pi^+$ backgrounds. Kinematic distributions in these events, especially events in which at least one charged particle is not correctly associated to the B candidate, are similar to each other, and also to those of other, poorly measured, charmless decays. We allow the overall event yield for this category of events to vary in the fit, after fixing the relative weight of each mode to the expected value [10,18]. The remaining events, which mostly originate from open $b \to c$ transitions, are parametrized as a separate background component, with its yield left free in the fit.

Table I summarizes the results of the fit. The $B^0 \to \rho^0\rho^0$ decay is observed with a significance of 3.1 standard deviations (σ), as determined by the quantity $\mathcal{S} = \sqrt{-2\ln(\mathcal{L}_0/\mathcal{L}_{\max})}$, where $\mathcal{L}_{\max}$ is the maximum likelihood value, and $\mathcal{L}_0$ is the likelihood for a fit with the signal contribution set to zero. Both likelihoods include systematic uncertainties, which are assumed to be Gaussian distributed and are discussed below. This significance level corresponds to a probability of 1.0×10^{-3} that the observed signal yield is consistent with a background fluctuation. We do not observe significant event yields for $B^0 \to \rho^0 f_0$ or $B^0 \to f_0 f_0$ decays, nor for the nonresonant decays $B^0 \to \rho^0\pi^+\pi^-$ and $B^0 \to \pi^+\pi^-\pi^+\pi^-$. We find 280 ± 53, 670 ± 96, 2329 ± 147, and $68\,701 \pm 281$ events for the $B^0 \to a_1^\pm\pi^\mp$, charmless, $b \to c$, and continuum backgrounds, respectively, consistent with expectations. In Fig. 1 we show the projections of the fit results onto m_{ES} and $m_{\pi\pi}$.

From the fit to the proper-time distribution of the data sample, we determine the CP-violating parameters

$$S_L^{00} = 0.3 \pm 0.7 \,(\text{stat.}) \pm 0.2 \,(\text{syst.}),$$

$$C_L^{00} = 0.2 \pm 0.8 \,(\text{stat.}) \pm 0.3 \,(\text{syst.})$$

for the longitudinal component of the $B^0 \to \rho^0\rho^0$ sample. The CP asymmetry projection is shown in Fig. 2. The statistical correlations between fit parameters for $B^0 \to \rho^0\rho^0$ are given in Table II.

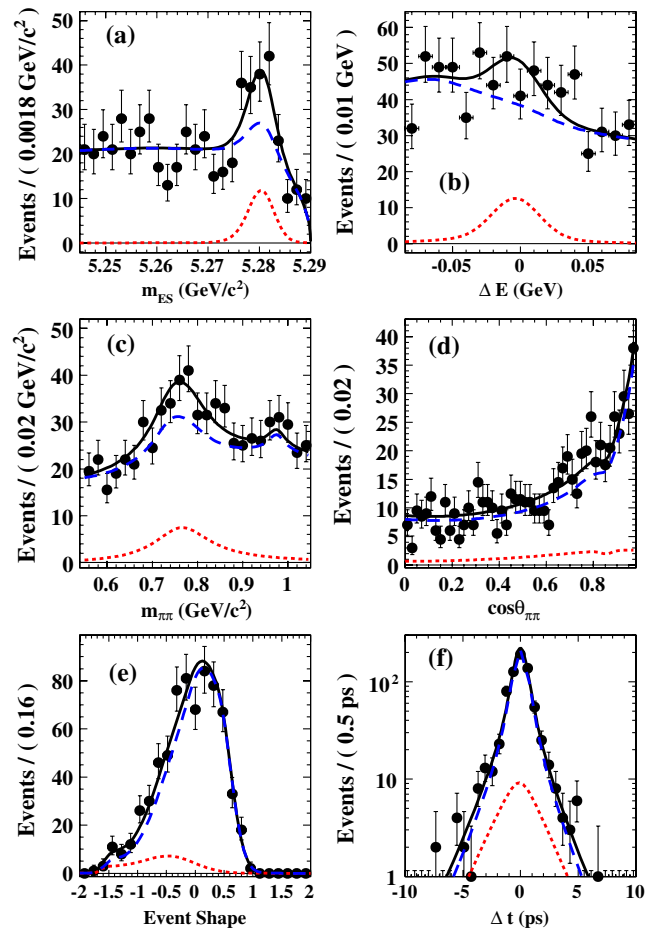FIG. 1 (color online). Projections of the multidimensional fit onto the (a) m_{ES}, (b) ΔE, (c) di-pion invariant mass $m_{\pi\pi}$ (average of m_1 and m_2 distributions is shown), (d) cosine of the helicity angle $\cos\theta_{\pi\pi}$ (average of $\cos\theta_1$ and $\cos\theta_2$ distributions is shown), (e) event shape discriminant $\mathcal{E}$, and (f) Δt, after a requirement on the signal-to-background probability ratio with the plotted variable excluded, which enhances the fraction of signal events in the sample. This selection has 40%–60% efficiency for signal, depending on the projection. The data points are overlaid by the full PDF projection (solid line). Also shown are the $B^0 \to \rho^0\rho^0$ PDF component (dotted line) and the sum of all other PDFs (dashed line).
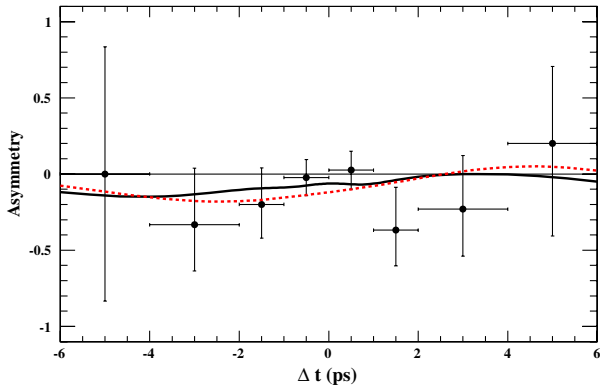
FIG. 2 (color online). CP asymmetry $\mathcal{A}_{CP}$ after a requirement on the signal-to-background probability ratio, which enhances the fraction of signal events in the sample. The solid line represents the projection of the total PDF; the dotted line is the $B^0 \to \rho^0\rho^0$ contribution.

Dominant systematic uncertainties in the fit originate from statistical errors in the PDF parametrizations due to the limited number of events in the control samples, variations in the B background branching ratios fixed in the fit, and from potential fit bias. The PDF parameters are varied by their respective uncertainties to derive the corresponding systematic errors. The fit bias is studied in a large number (~ 1000) of MC experiments, in which signal and dominant charmless B background events are fully simulated, while other backgrounds are sampled from their respective PDFs. We correct for the bias of 7.9 ± 2.0 events for $B^0 \to \rho^0\rho^0$, 0.00 ± 0.07 for C_L^{00}, and -0.02 ± 0.08 for S_L^{00}. The uncertainties associated with the B background model are 4 events for the signal yield, 0.01 for f_L, 0.01 for C_L^{00}, and 0.11 for S_L^{00}. The systematic uncertainties due to the charmless background composition, arising from the uncertainties in the individual branching ratios and the CP content of the B background [18,19], are 5 events for the signal yield, 0.01 for f_L, 0.18 for C_L^{00}, and 0.14 for S_L^{00}. The above systematic uncertainties do not scale with event yield and are included in the calculation of the significance of the result.

We estimate the systematic uncertainty due to the interference between all $B^0 \to 4\pi$ modes using simulated samples in which the decay amplitudes for $B^0 \to \rho^0\rho^0$, $B^0 \to \rho^0 f_0$, $B^0 \to f_0 f_0$, $B^0 \to \rho^0\pi^+\pi^-$, and $B^0 \to \pi^+\pi^-\pi^+\pi^-$ are generated according the measurements presented here, and those for $B^0 \to a_1^\pm\pi^\mp$ correspond to a

branching fraction of $(33.2 \pm 4.8) \times 10^{-6}$ [20]. The values of the individual branching ratios are varied within their respective uncertainties, and the strong phases and CP content of the interfering amplitudes are varied between zero and 2π using uniform distributions. We take the rms variation of the fitted values (14 events for the $\rho^0\rho^0$ yield, 0.04 for f_L, and 0.07 for S_L^{00} and C_L^{00}) as a systematic uncertainty. The interference with $B^0 \to a_1^\pm\pi^\mp$ is most important for $B^0 \to \rho^0\rho^0$ (14 events) and $B^0 \to \rho^0\pi^+\pi^-$ (13 events), while for the nonresonant modes, the largest effects are between $B^0 \to \rho^0\pi^+\pi^-$ and $B^0 \to \rho^0 f_0$ (9 events), and between $B^0 \to \pi^+\pi^-\pi^+\pi^-$ and $B^0 \to f_0 f_0$ (5 events).

Uncertainties in the reconstruction efficiency arise from track finding and particle identification, and are determined by dedicated studies on control data samples. Uncertainties due to other selection requirements, such as vertex probability, track multiplicity, and thrust angle, amount to 2.4% for the event yields, and are negligible for the polarization and CP observables.

We perform an isospin analysis of $B \to \rho\rho$ decays, by minimizing a χ^2 that includes the measured quantities expressed as the lengths of the sides of the isospin triangles [2]. We use the measured branching fraction and fraction of longitudinal polarization of $B^+ \to \rho^+\rho^0$ decays [6]; the measured branching fraction, polarization, and CP parameters S_L^{+-} and C_L^{+-} determined from the time evolution of the longitudinally polarized $B^0 \to \rho^+\rho^-$ decays [7]; and the branching fraction, polarization, and CP parameters S_L^{00} and C_L^{00} of $B^0 \to \rho^0\rho^0$ reported here. We assume uncertainties to be Gaussian distributed and neglect $I = 1$ isospin contributions, electroweak loop amplitudes, nonresonant, and isospin-breaking effects.

We obtain a 68% (90%) CL limit $|\alpha - \alpha_{\rm eff}| < 15.7°$ ($< 17.6°$) where $\alpha_{\rm eff}$ is defined by $\sin(2\alpha_{\rm eff}) = S_L^{+-}/(1 - C_L^{+-2})^{1/2}$. Figure 3 shows the confidence level with and without use of S_L^{00} and C_L^{00} in the isospin analysis. We observe four solutions near zero, as in the $B \to \pi\pi$ isospin

TABLE II.   Correlation matrix for $B^0 \to \rho^0\rho^0$ parameters.

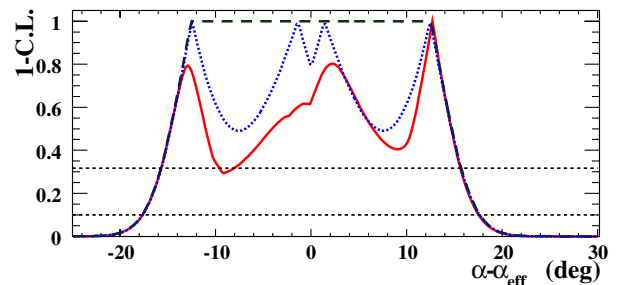| Parameter	Yield	f_L	S_L^{00}	C_L^{00}
Yield	1.000	0.086	-0.136	-0.273
f_L		1.000	-0.006	-0.174
S_L^{00}			1.000	-0.035
C_L^{00}				1.000

FIG. 3 (color online).   CL on $\alpha - \alpha_{\rm eff}$ determined from the isospin analysis. The long-dashed curve is obtained without the two CP parameters S_L^{00} and C_L^{00}. The dotted curve corresponds to the isospin analysis without S_L^{00}, and the solid curve CL includes both C_L^{00} and S_L^{00} in the fit. The horizontal dotted lines correspond to the 68% (top) and 90% (bottom) CL intervals.

analysis [21]. The additional constraint from S_L^{00} provides some discrimination among the four solutions.

In summary, we confirm our earlier evidence [4] for $B^0 \rightarrow \rho^0 \rho^0$ decays with a significance of 3.1σ and measure the branching fraction, longitudinal polarization fraction, and *CP* asymmetries in these decays. Our results are statistically consistent with the previous measurement [4] and supersede it. These measurements combined with those for $B^+ \rightarrow \rho^0 \rho^+$ and $B^0 \rightarrow \rho^+ \rho^-$ decays provide a constraint on the penguin uncertainty in the determination of the CKM unitarity angle α. Thus, this first measurement of the *CP* asymmetries in $B^0 \rightarrow \rho^0 \rho^0$ decays establishes the technique that, with significantly larger data sets, would help determine α with high precision. We find no significant evidence for the decays $B^0 \rightarrow \rho^0 f_0$, $B^0 \rightarrow f_0 f_0$, $B^0 \rightarrow \rho^0 \pi^+ \pi^-$, or $B^0 \rightarrow \pi^+ \pi^- \pi^+ \pi^-$.

Note added in proof.—After our paper was submitted, we became aware of the measurement [22] by the Belle Collaboration. Although Ref. [22] does not find significant evidence for $B^0 \rightarrow \rho^0 \rho^0$, the branching fractions are consistent with our results.

[1] N. Cabibbo, Phys. Rev. Lett. **10**, 531 (1963); M. Kobayashi and T. Maskawa, Prog. Theor. Phys. **49**, 652 (1973).

[2] M. Gronau and D. London, Phys. Rev. Lett. **65**, 3381 (1990).

[3] Charge conjugate decay modes are implied in this paper.

[4] B. Aubert *et al.* (*BABAR* Collaboration), Phys. Rev. Lett. **98**, 111801 (2007).

[5] J. Zhang *et al.* (Belle Collaboration), Phys. Rev. Lett. **91**, 221801 (2003).

[6] B. Aubert *et al.* (*BABAR* Collaboration), Phys. Rev. Lett. **97**, 261801 (2006).

[7] B. Aubert *et al.* (*BABAR* Collaboration), Phys. Rev. D **76**, 052007 (2007).

[8] A. Somov *et al.* (Belle Collaboration), Phys. Rev. Lett. **96**, 171801 (2006).

[9] A. F. Falk, Z. Ligeti, Y. Nir, and H. Quinn, Phys. Rev. D **69**, 011502(R) (2004).

[10] W.-M. Yao *et al.* (Particle Data Group), J. Phys. G **33**, 1 (2006).

[11] B. Aubert *et al.* (*BABAR* Collaboration), Nucl. Instrum. Methods Phys. Res., Sect. A **479**, 1 (2002).

[12] PEP-II Conceptual Design Report No. SLAC-R-418, 1993.

[13] B. Aubert *et al.* (*BABAR* Collaboration), Phys. Rev. Lett. **94**, 161803 (2005).

[14] D. Lange, Nucl. Instrum. Methods Phys. Res., Sect. A **462**, 152 (2001).

[15] The *BABAR* detector Monte Carlo simulation is based on GEANT4: S. Agostinelli *et al.*, Nucl. Instrum. Methods Phys. Res., Sect. A **506**, 250 (2003).

[16] E. M. Aitala *et al.* (E791 Collaboration), Phys. Rev. Lett. **86**, 765 (2001).

[17] B. Aubert *et al.* (*BABAR* Collaboration), Phys. Rev. Lett. **97**, 201801 (2006).

[18] E. Barberio *et al.* (Heavy Flavor Averaging Group), arXiv:0704.3575 and online update at http://www.slac.stanford.edu/xorg/hfag.

[19] B. Aubert *et al.* (*BABAR* Collaboration), Phys. Rev. Lett. **98**, 181803 (2007).

[20] B. Aubert *et al. BABAR* Collaboration, Phys. Rev. Lett. **97**, 051802 (2006).

[21] B. Aubert *et al.*, Phys. Rev. D **76**, 091102 (2007).

[22] C.-C. Chiang *et al.* (Belle Collaboration), arXiv: 0808.2576.